Research Square

Preprints are preliminary reports that have not undergone peer review.
They should not be considered conclusive, used to inform clinical practice,
or referenced by the media as validated information.

Site-specific fungal community shifts associated with continuous tomato cropping and Fusarium wilt symptoms in two contrasting greenhouse regions

Cai Yunfei

caiyf@zaas.ac.cn

Zhejiang Academy of Agricultural Sciences https://orcid.org/0000-0002-5077-5854

Jiali Ying

Youju Ye

Shuangshuang Wen

Renjuan Qian

Research Article

Keywords: Tomato, Elevation-associated environment, Soil microbial community, Continuous cropping, Fusarium oxysporum f. sp. lycopersici

Posted Date: November 24th, 2026

DOI: https://doi.org/10.21203/rs.3.rs-11608060/v1

License: This work is licensed under a Creative Commons Attribution 4.0 International License.
Read Full License

Type of the Paper (Research Article)

Site-specific fungal community shifts associated with continuous tomato cropping and Fusarium wilt symptoms in two contrasting greenhouse regions

Yunfei Cai[1], Jiali Ying[1], Youju Ye[1], Shuangshuang Wen[1], Renjuan Qian*[1]

[1]Zhejiang Institute of Subtropical Crops, Zhejiang Academy of Agricultural Sciences, Wenzhou, China, 325005.

Yunfei Cai, Email: caiyf@zaas.ac.cn;

Jiali Ying, Email: yingjl@zaas.ac.cn;

Youju Ye, Email: yeyj@zaas.ac.cn;

Shuangshuang Wen, Email: wenss@zaas.ac.cn;

Correspondence to:

Dr. Renjuan Qian, Zhejiang Institute of Subtropical Crops, Zhejiang Academy of Agricultural Sciences, Wenzhou, China.

Tel: 15957728225.

Email: qianrj@zaas.ac.cn

Postal address: Xueshan Road 334, Wenzhou 325005, P. R. China.

Abstract

Background and Aims

Continuous tomato monoculture frequently induces Fusarium wilt caused by *Fusarium oxysporum* f. sp. *lycopersici* (FOL). Soil bacterial and fungal communities jointly govern soil-borne disease development. Plateau and plain soils have distinct intrinsic properties, potentially leading to divergent microbiome responses and disease risks under monoculture. This study aimed to compare soil bacterial and fungal community shifts between plateau and plain tomato fields, and to link FOL abundance, microbiome alteration and wilt incidence.

Methods

Soil samples were collected from continuously cropped tomato fields in plateau and plain areas. Bacterial 16S rRNA and fungal ITS amplicon sequencing were analyzed on the Majorbio Cloud Platform. FOL absolute abundance was quantified using FOL-specific RT-qPCR, and field Fusarium wilt incidence was recorded.

Results

Continuous cropping restructured both bacterial and fungal communities in plateau and plain soils. Plain soil showed greater microbiome disruption, particularly in the fungal community. Although qPCR revealed no significant difference in FOL abundance between the two soils, plain fields exhibited markedly higher Fusarium wilt incidence. Several disease-associated microbial taxa were enriched in continuously cropped plain soil.

Conclusion

Higher wilt incidence in plain soil is not attributed to higher FOL abundance. Instead, the pronounced imbalance of the soil bacterial and fungal microbiome in plain soil facilitates disease outbreaks at comparable pathogen densities. This highlights that the overall soil microbiome status, rather than pathogen quantity alone, mediates Fusarium wilt risk under tomato monoculture.

Keywords: Tomato, Elevation-associated environment, Soil microbial community, Continuous cropping, *Fusarium oxysporum* f. sp. *lycopersici*

Introduction

Tomato (*Solanum lycopersicum*) is an economically important crop widely cultivated globally (Campos et al. 2021). However, continuous monoculture-related obstacles have become one of the major constraints to its sustainable production (Chellemi et al. 2012). Fusarium wilt is caused by the pathogen Fusarium oxysporum f. sp. lycopersici (FOL), long-term monoculture can increase disease risk and severity, resulting in substantial economic losses (Zhang et al. 2023). Soil microbial communities are essential for maintaining soil health and suppressing soil-borne diseases (Chellemi et al. 2012). Specific microorganisms, including *Pseudomonas*, *Bacillus*, and *Mortierella* species, have been shown to effectively restrict pathogen proliferation and infection in the soil (Weller et al. 2002; Xiong et al. 2017; Trivedi et al. 2020). In contrast, simplified microbial community structure and imbalanced function, particularly depletion of beneficial incidence (Trivedi et al. 2020). Elucidating microecological patterns linked to the of Fusarium wilt and exploring potential regulation strategies based on soil microbiome

features have become research hotspots.

The assembly and succession of soil microbial communities are regulated by multiple environmental factors. Elevation represents an integrated environmental gradient that combines temperature, precipitation, oxygen partial pressure, and soil physicochemical properties (Yao et al. 2025). Studies have shown that bacterial communities are primarily influenced by soil factors such as pH, whereas fungal communities are mainly affected by climatic factors including temperature and precipitation (Looby and Martin 2020; Ren et al. 2023). Sites above 3000 meters have reduced atmospheric oxygen partial pressure. Bacteria, leveraging their diverse metabolic capabilities, can maintain functional stability across different environmental conditions by adjusting community composition (Zhu et al. 2022; Li et al. 2024). In contrast, fungi, as strictly or facultatively aerobic eukaryotic microorganisms, possess respiratory chains highly dependent on oxygen, rendering them potentially sensitive to shifts in ambient oxygen availability (Maček 2022; Li et al. 2024). Most existing elevation-gradient microbial studies focus on natural ecosystems. Few observational field studies have combined pathogen molecular quantification to compare microbial community patterns under tomato continuous cropping between high-elevation and low-elevation agricultural sites. It remains unclear how soil microbiota composition correlates with crop performance and Fusarium wilt symptoms under contrasting field settings.

In this study, our study represents an observational field comparison across two geographically distinct greenhouse sites, rather than a fully factorial controlled experiment. We sampled continuously cropping and non-cropped soils at lowelevation (Zhejiang) and high-elevation (Sichuan) locations, combined with FOL-specific RT-qPCR pathogen quantification, to characterize differences in bulk-soil microbial communities and their associations with plant performance and Fusarium wilt symptoms. We

acknowledge that elevation is confounded with geographic location, soil parent material, and local management in our current sampling design, and we cannot isolate the independent causal effect of altitude. These observations provide baseline information for tomato production in plateau greenhouse systems.

Materials and methods

Field Sampling and Laboratory Analysis of Soil Chemical Characteristics

Soil sampling was performed in July 2023. Low-altitude soil samples (10 m a.s.l.) were collected from plot X (120°36′55″E, 27°58′01″N, plot size 450 m^2) in Ouhai District, Wenzhou City, Zhejiang Province, which had been subjected to three years of continuous tomato cropping, plot Y served as the local non-cropped control (plot size 300 m^2, adjacent to plot X). Plot Y had no tomato cultivation for ≥3 years, was fallow with sparse native weeds, and received no fertilization, irrigation or pesticide inputs for the duration of the tomato monoculture in plot X. The region is characterized by a subtropical monsoon climate, with an annual sunshine duration ranging from 1,442 to 2,264 hours.

High-altitude soil samples (3280 m a.s.l.) were collected from two spatially separated and managerially independent continuously-cropped tomato plots A and Q (plot size each ~400 m^2, minimum inter-plot distance 120 m) in Aba County, Aba Prefecture, Sichuan Province (101°42′E, 32°54′N). Both A and Q had undergone three years of continuous tomato cropping. Plot W was the corresponding local non-cropped control (plot size 350 m^2, fallow with plateau native weeds, no tomato, fertilizer or pesticide inputs for ≥3 years). The region experiences a continental plateau climate, receiving 2,000–2,200 hours of sunshine annually.

All greenhouses adopted identical target set-points for internal microclimate: ventilation and drip

irrigation systems maintained daytime temperatures between 20–28°C, nighttime temperatures above 13°C, and relative humidity between 45% and 50%. Tomato planting density was 2.8 plants m^{-2} across all greenhouse plots, the cultivar was ‘Zheyingfen 1’. Fertilizer rates, irrigation frequency and pesticide application schemes were harmonized according to local standard tomato production practices for each greenhouse site.

During the tomato flowering-fruiting period, soil sampling was performed within plots consistent cropping systems. Three composite bulk-soil samples were collected equidistantly along each plot diagonal from a depth of 5–20 cm and approximately 20 cm from the tomato plants. Each composite bulk-soil sample pooled soils collected surrounding ≥8 individual plants within the sampling zone. Visible debris (litter, stones, earthworms) were manually removed in the field, soils were homogenized and sieved through a 2-mm mesh. Processed soil was split into two subsamples: one stored immediately at −80 °C for microbiome analysis and pathogen RT-qPCR. The other air-dried for soil physicochemical measurement. The collected soils are bulk soils, not rhizosphere soils.

Analysis of soil chemical properties was conducted using standard published analytical protocols (Du et al. 2022; Dang et al. 2023). Measured parameters included pH, soil organic matter (SOM), total nitrogen (TN), total phosphorus (TP), total potassium (TK), along with available nitrogen (AN, determined by alkaline hydrolysis), available phosphorus (AP), and available potassium (AK).

For fruit phenotype measurements, 15 mature fruits from different individual plants were randomly harvested per plot for determination of fruit length, single-fruit weight, soluble sugar content and titratable acidity.

For disease rating scale. Fusarium wilt severity was scored on a 0–4 ordinal scale adapted from previously published scales for tomato Fusarium wilt. The rating criteria were as follows:

Rating	Symptom description
0	No visible symptoms; plant healthy
1	≤25% of leaves showing chlorosis or wilting
2	26–50% of leaves showing chlorosis or wilting
3	51–75% of leaves wilted; plant alive
4	>75% of leaves wilted, or plant dead

Disease incidence (DI%). The percentage of symptomatic plants (rating ≥ 1) was calculated per plot as:

$$\mathrm{DI\%} = \frac{N_{\mathrm{diseased}}}{N_{\mathrm{total}}} \times 100$$

Where N_{total}=20 plants per plot.

Disease index (DIX). A weighted severity index was calculated per plot using the general formula for ordinal disease scales:

$$\mathrm{DIX} = \frac{\sum_{i=0}^{4}(i \times n_i)}{4 \times N_{\mathrm{total}}} \times 100$$

where i is the disease rating, n_i is the number of plants assigned to rating i, and 4 is the maximum rating on the scale. DIX ranges from 0 to 100. The use of this weighted index is preferred over incidence alone because it retains information on the severity distribution within a plot, not merely the presence or absence of disease.

FOL-specific RT-qPCR

Total soil DNA for RT-qPCR was extracted from 0.5 g frozen bulk soil using OMEGA Soil DNA Kit (D5625-01). Pathogen *Fusarium oxysporum* f. sp. *lycopersici* (FOL) was quantified using race-1 specific primer set Fol-F / Fol-R targeting SIX1 effector gene (Rep et al. 2004), which is specific to FOL

pathogenic isolates. The RT-qPCR reaction (20 μL total): 10 μL 2×SYBR Green RT-qPCR Master Mix, 0.4 μL forward primer (10 μM), 0.4 μL reverse primer (10 μM), 1 μL template soil DNA, 8.2 μL nuclease-free water. RT-qPCR thermal profile: 95 °C for 3 min; 40 cycles of 95 °C 10 s, 60 °C 30 s; followed by melting-curve analysis (65 °C–95 °C) to verify amplification specificity.

Standard curve was constructed using serial dilutions of plasmid containing cloned SIX1 gene fragment. The amplification efficiency was 96.7%, $R^2 = 0.994$. FOL target gene copy numbers per gram dry soil were calculated for each sample. Each DNA sample was run in two technical replicates.

DNA extraction, PCR amplification, and sequencing

Total microbial DNA was isolated from frozen soil samples using the OMEGA Soil DNA Kit (D5625-01; Omega Bio-Tek, Norcross, GA, USA). DNA quality was checked by agarose gel electrophoresis and spectrophotometry. Sterile water was used as a negative control to monitor contamination. The bacterial 16S rRNA gene (V3–V4 region) and the fungal ITS1 region were amplified using primer sets 338F/806R and 1737F/2043R, respectively (Cui et al. 2025).

Each 25-μL PCR reaction contained: 5 μL of 5×reaction buffer, 5 μL of 5×GC buffer, 2 μL of dNTPs (2.5 mmol L^{-1}), 1 μL each of forward and reverse primers (10 μmol L^{-1}), 2 μL of DNA template, 8.75 μL of ddH_2O, and 0.25 μL of Q5 DNA Polymerase (5 U μL^{-1}). The amplification program included an initial denaturation at 98 °C for 5 min; 30 cycles of 98 °C for 30 s, 55 °C for 30 s, and 72 °C for 45 s; and a final extension at 72 °C for 5 min, concluding with 4 °C hold.

PCR amplicons were checked via 0.8% agarose gel electrophoresis. Qualified products were sequenced on Illumina NovaSeq6000 platform at Shanghai Pansino Biotechnology Co., Ltd. Raw sequencing data have been deposited in the NCBI BioProject :

16S (https://dataview.ncbi.nlm.nih.gov/object/PRJNA1433159?reviewer=in31qt2e1j0ibr4chbm472ce95), ITS (https://dataview.ncbi.nlm.nih.gov/object/PRJNA1432652?reviewer=p3auvd8ifur8kki4rqtohobdd1).

Bioinformatics Analysis of Sequencing Data

Raw fastq data were processed on the Majorbio Cloud Platform (https://www.majorbio.com). Paired-end reads were quality-filtered, primers were trimmed, denoised to generate amplicon sequence variants (ASVs) using DADA2, chimeric sequences were identified and removed. Taxonomic annotation: bacterial 16S against Greengenes v13.8 database; fungal ITS against UNITE v8.3 database. Taxonomy assignment confidence threshold = 0.7. Non-target host sequences and low-abundance ASVs (cumulative count < 5 across all samples) were filtered out. Sequences were rarefied to uniform sequencing depth prior to downstream alpha- and beta-diversity calculation.

Note: The reported ASV counts (47 bacterial ASVs,17 fungal ASVs) refer to shared ASVs shown in Venn diagram (Figure2a-b), not total ASVs across the whole dataset. Total observed ASVs in the full dataset were substantially higher.

Microbial Diversity Analysis

Alpha-diversity indices (ACE, Chao1, Shannon, Simpson) were calculated on rarefied ASV tables using Majorbio cloud built-in functions, and visualizations were generated with R package "ggplot2".

Beta-diversity: Bray–Curtis dissimilarity (Bray and Curtis 1957) with the "ape" package. PERMANOVA (adonis2, R-vegan) with 9999 permutations was used to test community compositional differences across plots, permutations were constrained within plot grouping to account for nested

sampling structure; multivariate homogeneity of group dispersion was tested with "betadisper".

Classification of taxa into Transient / Intermittent / Persistent was performed according to (Liu et al. 2024): taxa present in < 33%, 33-66%, > 66% of samples within a given plot group were defined as Transient, Intermittent, Persistent respectively. We acknowledge the limited statistical robustness of this classification given n=3 composite samples per plot.

Statistical Comparisons

IBM SPSS Statistics 26 was used for univariate statistics, including one-way ANOVA for soil properties, alpha-diversity indices and FOL RT-qPCR gene copy numbers, followed by LSD post-hoc test ($p < 0.05$). Tukey's HSD was employed for additional pairwise comparisons. Results are presented as means ± standard error (SE), bar charts show means ± standard deviation (SD), n= 3 composite samples per plot.

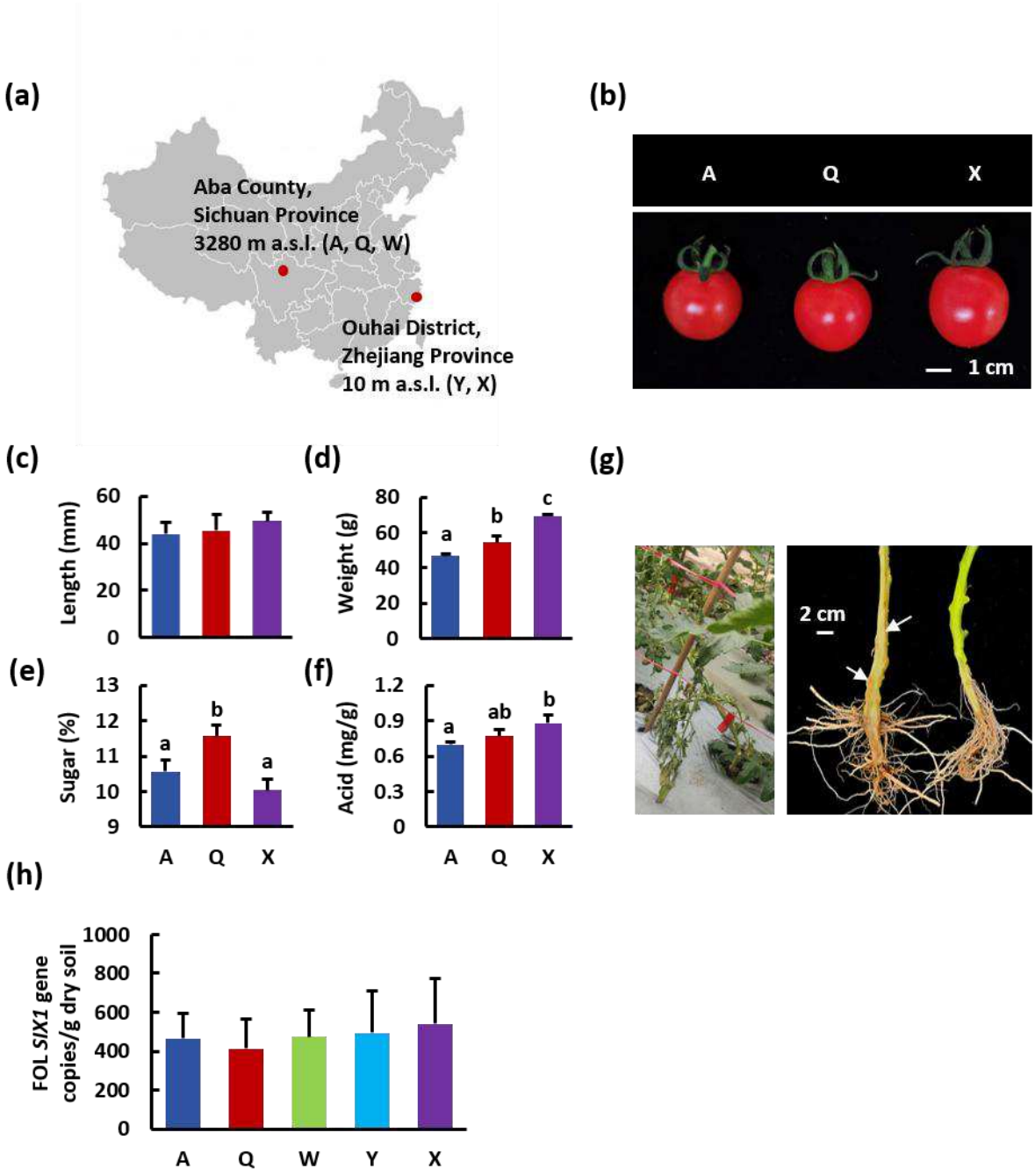
Results

Low-altitude continuously cropped plot X exhibited Fusarium wilt symptoms

To determine crop performance, plant health and pathogen abundance under two geographically distinct greenhouse regions, we selected two continuously-cropped plots A and Q at high elevation (3280 m a.s.l., Sichuan) and one continuously-cropped plot X at low elevation (10m a.s.l., Zhejiang), all planted with tomato variety ‘Zheyingfen 1’ (Figure 1a). Plots W and Y represented corresponding local non-cropped fallow controls. We observed phynotypic differences across plots (Figure 1b). Fruit length showed no significant difference among plots A, Q, and X (Figure 1c). Plot X produced significantly heavier than that from plots A and Q, and plot Q had heavier fruits than A (Figure 1d). Soluble sugar content was

207 significantly higher in Q than in A and X (Figure 1e). Acidity was significantly higher in X relative to A

208 and Q (Figure 1f).



209 **Figure 1 Continuous Tomato Cropping leads to Fusarium wilt symptoms in low-elevation plot X.**

210 Corrected sampling-plot geographic assignment: high-elevation plots A, Q, W (Aba County, 3280 m

211 a.s.l.); low-elevation plots X, Y (Ouhai District, 10 m a.s.l.) (a). Fruit morphology of 'Zheyingfen 1'

212 tomato in plots A, Q, and X (b). Statistical results of tomato fruit length (c), weight (d), sugar content (e),

and acidity (f). Typical Fusarium-wilt-symptomatic plant in plot X; white arrows show vascular browning (g). FOL-SIX1 RT-qPCR pathogen gene copies per gram dry bulk soil across plots (h). Different letters denote significant differences at $p < 0.05$. Bars represent mean ± SD ($n = 3$ composite samples).

We recorded the occurrence of tomato Fusarium wilt in different plots (Table S1) and calculated the disease index for each plot (Table S2). Based on the mean disease incidence (Table 1), tomato Fusarium wilt was severe in plot X, whereas it was essentially absent in plots A and Q. Typical vascular-browning Fusarium wilt symptoms were visually observed on tomato plants in plot X after three years of continuous cropping (Figure 1g). We used FOL-specific RT-qPCR targeting the SIX1 effector gene to quantify pathogenic FOL copy numbers in soil. Although plot X had slightly higher FOL gene copy numbers per gram of dry soil than plots A, Q, W, and Y, analysis of variance (ANOVA) showed no statistically significant differences among the plots (Figure 1h).

Table 1 Mean disease incidence of Fusarium wilt in plots A, Q and X

Plots	Diseased plants / total assessed	DI (%) (mean ± SEM)	Range (%)
A	**2/80**	**2.5 ± 1.44**	**0.00-5.00**
Q	**3/80**	**3.75 ± 2.39**	**0.00–10.00**
X	**59/80**	**73.75 ± 4.27**	**65.00–85.00**

Soil nutrient differences

To evaluate whether soil physicochemical differences could explain plant symptom differences, we measured soil properties across plots A, Q, W, X, and Y (Table 2). No significant inter-plot differences

were detected for pH, TN, TP, TK, AN, AP, and AK. Soil organic matter (SOM) in plot X was significantly lower than that in A, Q, W, and Y. Greenhouse microclimate set-points were harmonized across sites. We note that multiple unmeasured co-varying environmental differences exist between the two geographic locations, including ambient oxygen partial pressure, baseline soil formation background, and other site-specific factors.

Table 2 Differences in soil properties among different plots

Indicators	A	Q	W	Y	X
pH	7.37 ± 0.43a	7.29 ± 0.37a	7.34 ± 0.33a	6.93 ± 0.41a	6.87± 0.39a
SOM (g/kg)	22.47 ± 3.45a	23.54 ± 4.13a	21.53 ± 2.95a	19.37 ± 5.21a	16.49 ± 4.36b
TN (g/kg)	1.54 ± 0.29a	1.47 ± 0.35a	1.49 ± 0.31a	1.17 ± 0.34a	1.28 ± 0.43a
TP (g/kg)	2.49 ± 0.67a	1.95 ± 0.75a	2.38 ± 0.59a	3.21 ± 0.51a	2.93 ± 0.39a
TK (g/kg)	29.53 ± 0.44a	27.79 ± 0.65a	27.63 ± 0.59a	25.48 ± 0.37a	23.63 ± 0.72a
AN (mg/kg)	74.56 ± 20.27a	92.54 ± 19.72a	98.62 ± 25.94a	117.57 ± 17.26a	106.98 ± 37.87a
AP (mg/kg)	342.56 ± 69.47a	383.17 ± 48.62a	366.58 ± 67.29a	379.49 ± 85.39a	381.26 ± 79.55a
AK (mg/kg)	667.57 ± 145.94a	628.34 ± 117.46a	599.76 ± 184.85a	654.77 ± 214.67a	683.97 ± 227.52a

Microbiome data acquisition and analysis

Fungal ITS and bacterial 16S rRNA V3–V4 amplicons were sequenced for the 15 composite bulk-soil samples. Total of 443,760 high-quality bacterial sequences and 711,644 high-quality fungal sequences

were obtained. The Venn diagram (Figure 2a, b) displays shared and unique ASVs among the five plot groups, rather than total dataset-wide ASVs. Among group-shared ASVs, 27 out of 47 bacterial ASVs were shared (57.45%); 7 out of 17 fungal group-shared ASVs were shared (41.18%).

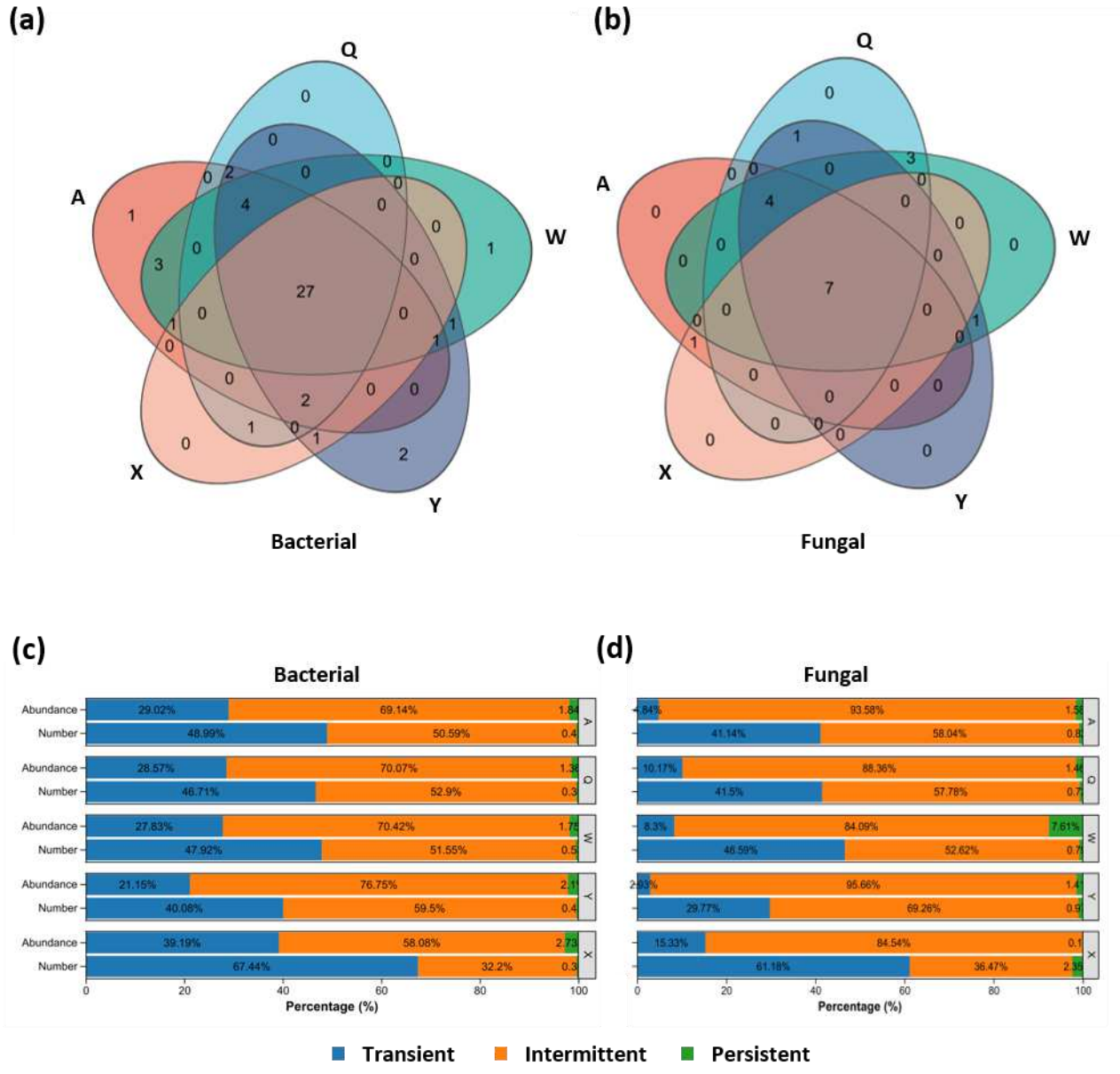


Figure 2 Comparison of environmental sensitivity of soil microbial communities in high-altitude and low-altitude regions. Venn diagram of shared-group ASVs for soil bacteria (a) and fungi (b). Note that Venn shows shared-group ASVs rather than total dataset ASVs. Community composition classified by detection prevalence: Transient (<33% detection within plot-group), Intermittent (33–66%), Persistent

(>66%). Bacteria (c) and fungi (d). Abscissa is percentage; ordinate is mean relative abundance or proportion of detected ASVs. Caution: classification robustness is limited given n=3 composite samples per plot.

Community composition based on prevalence reveals the unique microbial distribution pattern in plot X

Taxa classified as Transient, Intermittent, and Persistent based on their prevalence in the samples for analysis (Liu et al. 2024). Among these, Intermittent bacteria dominated both relative abundance and detected ASV count proportion. In plot X, Transient and Intermittent bacteria co-dominated (Figure 2c).

For fungi, Intermittent taxa dominated relative abundance in A, Q, W, Y. In plot X, Intermittent fungi represented high relative abundance but low proportion of total detected ASVs. Transient fungi had low relative abundance yet accounted for most detected ASVs (Figure 2d). This represents a distinct community prevalence pattern in plot X compared with other plots.

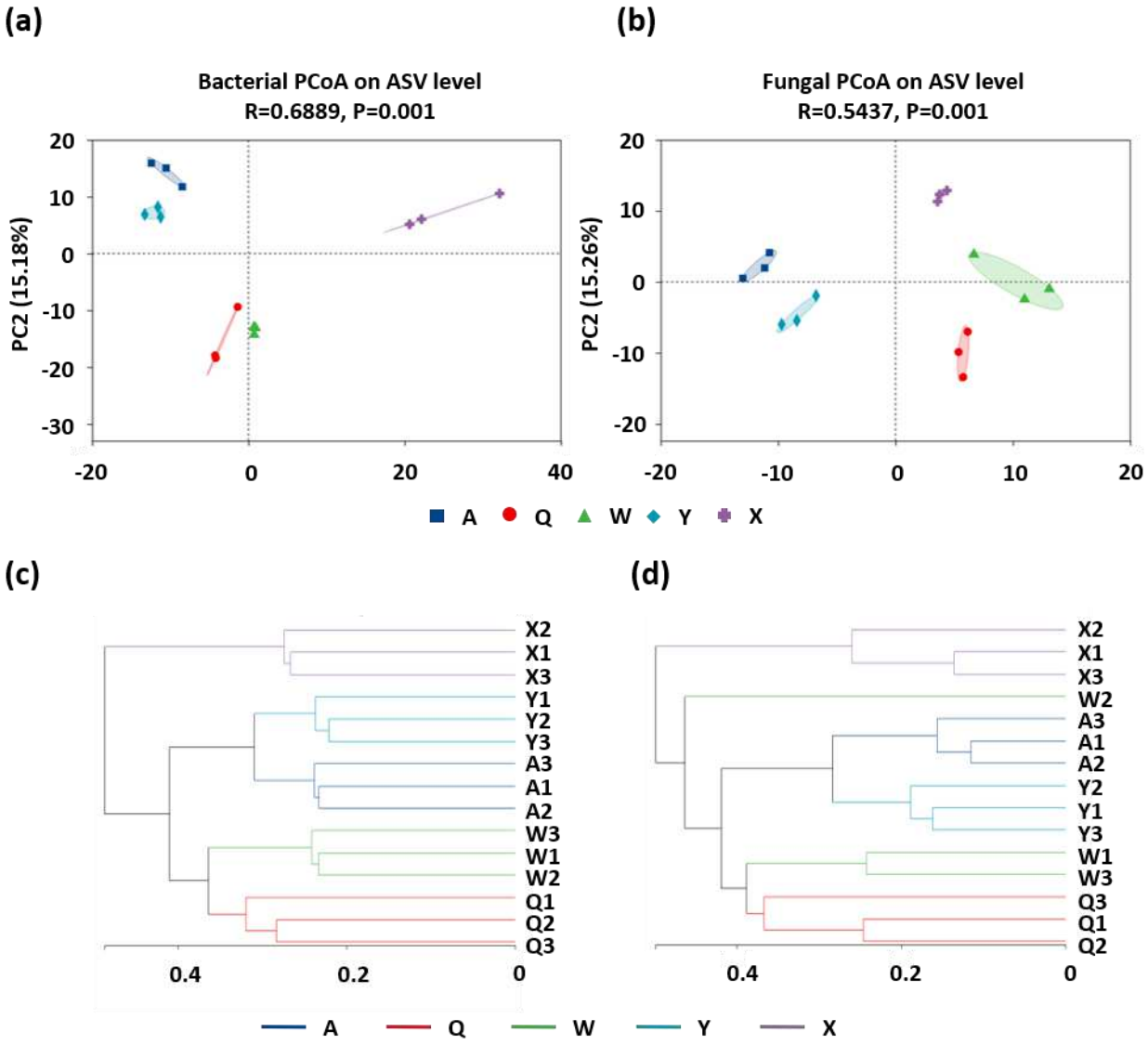
Further validation of the unique microbial pattern in plot X by alpha and beta diversity

Alpha diversity indices were analyzed to quantify the impact of the distribution pattern on community internal structure (Table 3). For bacteria, ACE, Chao1, and Shannon indices in plot X were comparable to other plots, and Simpson index showed moderate differences. In contrast, fungal communities in plot X displayed consistently lower ACE, Chao1, and Shannon indices than other plots, indicating lower fungal richness and diversity.

Table 2 Differences in soil alpha diversity index

Microbiome	Samples	ACE	Chao1	Shannon	Simpson
Bacteria	A	1433.2 ± 190.2a	1434.1 ± 190.8a	6.7 ± 0.1a	0.0023 ± 0.1a
	Q	1369.9 ± 316.6a	1370.4 ± 317.3a	6.5 ± 0.4a	0.0059 ± 0.1d
	W	1140.2 ± 17.4a	1140.0 ± 17.3b	6.5 ± 0.1a	0.0024 ± 0.1a
	Y	1425.8 ± 51.9a	1426.3 ± 51.6a	6.6 ± 0.1a	0.0028 ± 0.1b
	X	1291.5 ± 263.0a	1290.9 ± 262.5a	6.5 ± 0.1a	0.0034 ± 0.1c
Fungi	A	244.8 ± 24.0a	244.9 ± 24.0a	3.5 ± 0.1a	0.0904 ± 0.1a
	Q	244.8 ± 44.9a	244.9 ± 44.8a	3.5 ± 0.6a	0.0904 ± 0.1a
	W	254.5 ± 92.0a	254.3 ± 92.0a	2.9 ± 1.4b	0.2682 ± 0.3b
	Y	206.2 ± 29.6b	206.1 ± 29.5b	3.4 ± 0.4a	0.0854 ± 0.1a
	X	56.7 ± 15.1c	56.7 ± 15.0c	1.6 ± 0.1c	0.3727 ± 0.1b

PCoA based on Bray-Curtis dissimilarity showed that in the bacterial community, sample points from plot X were clearly separated from those of other plots for both bacterial and fungal communities (Figure 3a, b). PERMANOVA confirmed significant community compositional differences across plots. Hierarchical clustering further supported distinct community profiles for plot X bulk-soil samples (Figure 3c-d).



280 **Figure 3 Soil microbial communities in low-elevation plot X are distinct under continuous tomato**

281 **cropping.** PCoA based on Bray-Curtis dissimilarity for bacterial community (a) and fungal community

282 (b). Each point represents one composite soil sample. PERMANOVA (adonis2, constrained permutations,

283 9999 permutations) and betadisper were applied to test community-level difference and multivariate

284 dispersion. Hierarchical clustering based on Bray-Curtis distance for bacteria (c) and fungi (d).

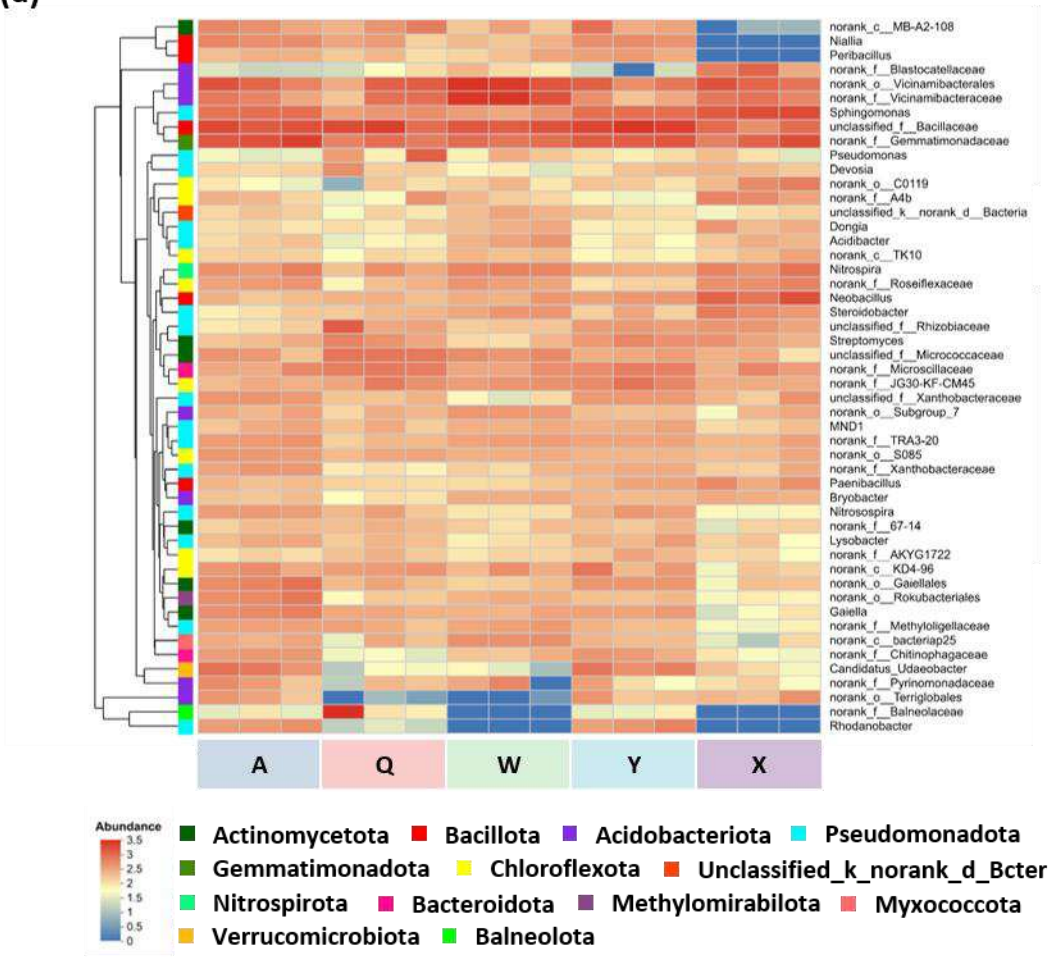
Bacterial and fungal community differences across plots under continuous tomato cropping

Heatmap visualization of dominant genera indicated minor differences for bacterial communities. Genera *norank_f_Baineolaceae*, *norank_c_MB-A2-108*, *Niallia*, and *Peribacillus* showed reduced abundance in plot X (Figure 4a).

For fungi communities, high-altitude plots A, Q, W, and the low-altitude non-cropped Y displayed similar genus-level profiles. In plot X, most fungal genera declined in relative abundance, while *unclassified_f_Microascaceae*, *Conocybe*, *Curvularia*, *Exserohilum,* and *Cephaliophora* increased (Figure 4b). The ITS-based relative abundance of *Fusarium* genus was not markedly elevated in plot X (Figure 4b). However, as many other fungal taxa decreased, *Fusarium* occupied a higher proportional fraction within the disturbed fungal community of plot X.

296

(a)


norank_c__MB-A2-108
Niallia
Peribacillus
norank_f__Blastocatellaceae
norank_o__Vicinamibacterales
norank_f__Vicinamibacteraceae
Sphingomonas
unclassified_f__Bacillaceae
norank_f__Gemmatimonadaceae
Pseudomonas
Devosia
norank_o__C0119
norank_f__A4b
unclassified_k__norank_d__Bacteria
Dongia
Acidibacter
norank_c__TK10
Nitrospira
norank_f__Roseiflexaceae
Neobacillus
Steroidobacter
unclassified_f__Rhizobiaceae
Streptomyces
unclassified_f__Micrococcaceae
norank_f__Microscillaceae
norank_f__JG30-KF-CM45
unclassified_f__Xanthobacteraceae
norank_o__Subgroup_7
MND1
norank_f__TRA3-20
norank_o__S085
norank_f__Xanthobacteraceae
Paenibacillus
Bryobacter
Nitrosospira
norank_f__67-14
Lysobacter
norank_f__AKYG1722
norank_c__KD4-96
norank_o__Gaiellales
norank_o__Rokubacteriales
Gaiella
norank_f__Methyloligellaceae
norank_c__bacteriap25
norank_f__Chitinophagaceae
Candidatus_Udaeobacter
norank_f__Pyrinomonadaceae
norank_o__Terriglobales
norank_f__Balneolaceae
Rhodanobacter
A
Q
W
Y
X
Abundance
3.5
3
2.5
2
1.5
1
0.5
0
Actinomycetota
Bacillota
Acidobacteriota
Pseudomonadota
Gemmatimonadota
Chloroflexota
Unclassified_k_norank_d_Bcter
Nitrospirota
Bacteroidota
Methylomirabilota
Myxococcota
Verrucomicrobiota
Balneolota

(b)

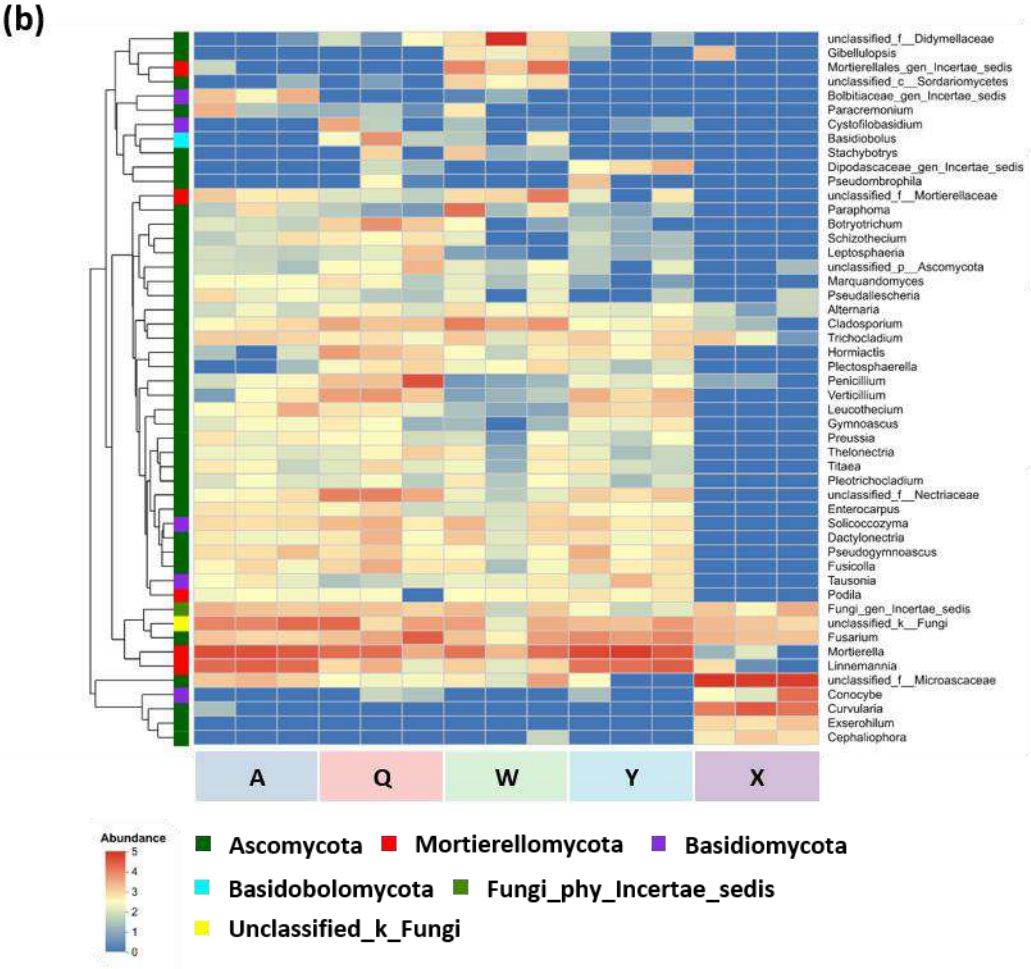

unclassified_f__Didymellaceae
Gibellulopsis
Mortierellales_gen_Incertae_sedis
unclassified_c__Sordariomycetes
Bolbitiaceae_gen_Incertae_sedis
Paracremonium
Cystofilobasidium
Basidiobolus
Stachybotrys
Dipodascaceae_gen_Incertae_sedis
Pseudombrophila
unclassified_f__Mortierellaceae
Paraphoma
Botryotrichum
Schizothecium
Leptosphaeria
unclassified_p__Ascomycota
Marquandomyces
Pseudallescheria
Alternaria
Cladosporium
Trichocladium
Hormiactis
Plectosphaerella
Penicillium
Verticillium
Leucothecium
Gymnoascus
Preussia
Thelonectria
Titaea
Pleotrichocladium
unclassified_f__Nectriaceae
Enterocarpus
Solicoccozyma
Dactylonectria
Pseudogymnoascus
Fusicolla
Tausonia
Podila
Fungi_gen_Incertae_sedis
unclassified_k__Fungi
Fusarium
Mortierella
Linnemannia
unclassified_f__Microascaceae
Conocybe
Curvularia
Exserohilum
Cephaliophora
A
Q
W
Y
X
Abundance
5
4
3
2
1
0
Ascomycota
Mortierellomycota
Basidiomycota
Basidobolomycota
Fungi_phy_Incertae_sedis
Unclassified_k_Fungi

Figure 4 Heatmap of dominant bacterial and fungal genera across plots under continuous tomato cropping. Heatmap showing the relative abundance of dominant bacterial (a) and fungal (b) genera in soil samples from different altitudinal plots under continuous tomato cropping. The color gradient from blue to red represents low to high relative abundance. Note: the genera shown in this heatmap were annotated from all ASVs in the full dataset, not only the 17 shared-group fungal ASVs shown in the Venn diagram (Figure 2b).

Multi-group comparison by ANCOM-BC

Multi-group comparison (ANCOM-BC, adjusted $p < 0.05$) identified differentially abundant taxa (Lin and Peddada 2020). For bacteria, *Sphingomonas*, *Neobacillus* were enriched in certain plots, *norank_o_Gaiellales*, *Gaiella*, and *Niallia* decreased in plot X (Figure 5a).

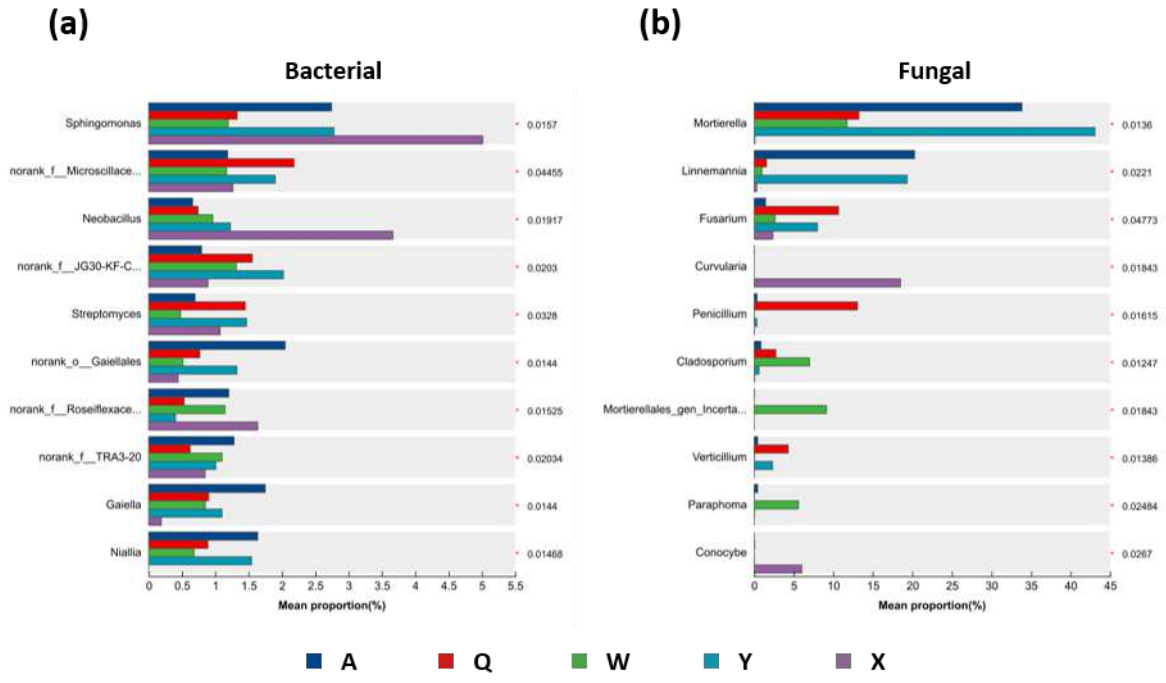


Figure 5 Multi-group comparison (ANCOM-BC, adjusted p<0.05) of microbial genera across plots. Bacteria (a); fungi (b). Y-axis: taxonomic genus names; X-axis: relative-abundance percentage. Colour corresponds to plot group. Significance markers: * $0.01<p\leq0.05$; ** $0.001<p\leq0.01$; *** $p \leq0.001$.

For fungi, *Curvularia* and *Conocybe* in plot X were significantly higher than in other plots, while those of *Mortierella*, *Linnemannia*, *Penicillium*, *Cladosporium*, *Mortierellales_gen_Incertae_sedis*, *Verticillium*, and *Paraphoma* were significantly lower (Figure 5b). The relative genus-level abundance of *Fusarium* in plot X was lower than in plots Q and Y, similar to that in plot W, and lowest in plot A. These observations show that plot X was characterized by depletion of many fungal taxa and enrichment of a small set of opportunistic fungi, resulting in strong compositional reshaping of the fungal assemblage.

Discussion

Elevation-associated environments integrate temperature, solar radiation, diurnal temperature fluctuation, atmospheric partial pressure of oxygen, soil parent material and local management practices. In this observational study, greenhouse microclimate set-points for temperature and humidity were harmonized between the two geographically separated sites, yet many other site-specific confounding variables could not be experimentally disentangled. Bacterial community composition showed relatively moderate shifts across plots; only a small subset of bacterial genera differed in plot X, supporting the view that soil bacterial assemblages possess relatively high compositional buffering capacity (Figure 4a). In contrast, the fungal community in plot X underwent pronounced compositional restructuring, with reduced richness and diversity (Figure 4b). Our observations are consistent with previous reports that fungi may be more sensitive to site-specific environmental shifts compared with bacteria. However, our sampling was limited to one low-elevation continuously cropped plot and two high-elevation plots from distinct geographic zones, so it may be premature to attribute the shifts in fungal communities solely to altitude or soil oxygen availability.

Using RT-qPCR targeting the *SIX1* effector gene of FOL, we detected a slightly higher copy number

of the pathogenic FOL gene in the soil of symptomatic plot X than in the other plots, although this difference did not reach statistical significance (Figure 1h). This molecular evidence confirmed the presence of pathogenic FOL in the soil of plot X. Meanwhile, the proportion of Fusarium in the fungal community was relatively high, which may be mainly attributable to a sharp decline in coexisting fungal taxa rather than a large-scale expansion of the pathogenic FOL population (Figure 5b). At the high-elevation site, continuously cropped plots A and Q retained relatively high relative abundance of fungal genera such as *Mortierella* and *Penicillium* (Figure 5b). In plot X from the low-elevation site, continuous tomato cropping was associated with severe simplification of the bulk-soil fungal community, depletion of multiple fungal taxa, and enrichment of several opportunistic fungal genera (Figure 4b and 5b). These community changes co-occurred with visual Fusarium wilt symptoms on tomato plants in plot X.

Previous studies have shown that various soil fungal groups, including *Mortierella* and *Penicillium*, may contribute to the soil's disease-suppressive capacity. Studies have shown that the rhizosphere of healthy plants is enriched with potentially beneficial microbiota and that non-pathogenic Fusarium species compete ecologically with pathogens (Chellemi et al. 2012). The decline of these fungal groups in the soil of plot X may be associated with the occurrence of Fusarium wilt symptoms in this plot. Although pathogenic FOL was detected by RT-qPCR, its absolute gene copy number was not statistically significantly higher than in the other plots (Figure 1h). However, because of the sharp decline in coexisting fungal groups, Fusarium accounted for a larger proportion of the disturbed fungal community in plot X (Figure 5b). This offers a possible explanation for the field observation that obvious wilt symptoms occurred without a significant increase in FOL pathogen abundance.

We acknowledge several important limitations of this field observational study. Altitude is closely

intertwined with geographic location, soil background, and site-specific history, so the independent effects of altitude cannot be disentangled in this design; reciprocal soil-transplant common-garden experiments with multiple independent sites per elevation would be needed to test causal hypotheses. Only one low-elevation continuously cropped plot, plot X, was available for sampling, while two spatially independent continuous-cropping plots, A and Q, were sampled at high elevation, which makes the replication structure unbalanced. The non-cropped fallow controls differ not only in cropping history but also in plant rhizodeposition input, and ideal controls would include first-year tomato or crop-rotation soils. The soils collected were bulk soil sampled 20 cm away from plant stems rather than rhizosphere soil. Visual Fusarium wilt symptoms were observed, and disease incidence and disease index were quantified per plot using a 0–4 ordinal scale (Table S1; Table S2). Finally, soil oxygen was not directly measured. Therefore, it remains unclear whether the occurrence of wilt disease in plot X was caused by differences in soil oxygen availability, namely through an imbalance in the microbial community of this plot that subsequently led to a disruption of the fungal community.

In addition, A key limitation of the present observational design is that elevation, geographical location, and management history are confounded, so the causal drivers of the observed differences cannot be resolved. Future research should therefore conduct reciprocal soil-transplant and common-garden experiments at multiple independent sites across different elevations. Such designs would allow soils and plants to be exchanged among sites while controlling for local environmental conditions, thereby helping to disentangle the effects of elevation, site-specific soil properties, and continuous-cropping history on fungal community assembly and Fusarium wilt symptoms.

In summary, this work documents strong site-specific bulk-soil fungal community restructuring associated with continuous tomato monoculture and Fusarium wilt symptoms in a low-elevation

greenhouse plot. FOL-specific RT-qPCR confirmed the presence of pathogenic FOL in symptomatic plot-X soil, without statistically significant elevation of pathogen gene copies compared with other plots. Bacterial communities showed comparatively minor changes. The environmental drivers underlying the observed microbial differences remain unresolved and require further targeted experimentation. Our dataset supplies observational microecological background information for tomato continuous-cropping research across contrasting plain and plateau greenhouse production systems.

Contributions

Yunfei Cai: Formal Analysis, Investigation, Validation, Writing – Original Draft. Jiali Ying: Writing – Review & Editing. Youju Ye: Software, Writing – Original Draft. Shuangshuang Wen: Formal Analysis, Investigation. Renjuan Qian: Conceptualization, Funding acquisition, Methodology, Writing - Review & Editing, Supervision.

Data availability statement

All data generated or analysed during this study are included in this published article and its supplementary information files.

Conflict of interests

The authors declare that they have no known competing financial interests or personal relationships that could have appeared to influence the work reported in this paper.

Fundings

This work was supported by Zhejiang Leading Talents Program (2024C04006), A Specific Program of

the Industry Technology Service Team at Ouhai Science and Innovation Center (OHKC2024003), and Wenzhou Scientific Research Project (X2023104).

References

Bray JR, Curtis JT (1957) An Ordination of the Upland Forest Communities of Southern Wisconsin. Ecological Monographs 27:325–349. https://doi.org/10.2307/1942268

Campos MD, Félix MDR, Patanita M, et al (2021) High throughput sequencing unravels tomato-pathogen interactions towards a sustainable plant breeding. Horticulture Research 8:171. https://doi.org/10.1038/s41438-021-00607-x

Chellemi DO, Wu T, Graham JH, Church G (2012) Biological Impact of Divergent Land Management Practices on Tomato Crop Health. Phytopathology® 102:597–608. https://doi.org/10.1094/PHYTO-08-11-0219

Cui Y, Ning Z, Li M, et al (2025) Microbial network-driven remediation of saline-alkali soils by salt-tolerant plants. Front Microbiol 16:1565399. https://doi.org/10.3389/fmicb.2025.1565399

Dang K, Ji L, Slaughter LC, et al (2023) Synergistic changes of rhizosphere bacterial community and soil properties in greenhouse soils under long-term tomato monoculture. Applied Soil Ecology 183:104738. https://doi.org/10.1016/j.apsoil.2022.104738

Du J, Song B, Jia Q, et al (2022) Effect of long-term sugar beet cultivation on rhizosphere bacterial diversity, community structure and sugar yield of sugar beet. Rhizosphere 22:100507. https://doi.org/10.1016/j.rhisph.2022.100507

Li Y, Chen Z, Zhang N, et al (2024) Decreased microbial phylogenetic diversity and community stability due to less bioavailable carbon and greater oxygen supply in Mollisols along a cultivation chronosequence. Soil and Tillage Research 238:106005. https://doi.org/10.1016/j.still.2024.106005

Lin H, Peddada SD (2020) Analysis of compositions of microbiomes with bias correction. Nat Commun 11:3514. https://doi.org/10.1038/s41467-020-17041-7

Liu H-Q, Li H-J, Li S-C, Xiang Y-Z (2024) Differentiation strategies for microbial community assembly and their associations with soil functions in lemon farmland. Applied Soil Ecology 201:105493. https://doi.org/10.1016/j.apsoil.2024.105493

Looby CI, Martin PH (2020) Diversity and function of soil microbes on montane gradients: the state of knowledge in a changing world. FEMS Microbiology Ecology 96:fiaa122. https://doi.org/10.1093/femsec/fiaa122

Maček I (2022) Fungi in Hypoxic Soils and Aquatic Sediments. In: Sahay S (ed) Extremophilic Fungi.

Springer Nature Singapore, Singapore, pp 219–243

Ren Z, Ye S, Li H, et al (2023) Biological Interactions and Environmental Influences Shift Microeukaryotes in Permafrost Active Layer Soil Across the Qinghai-Tibet Plateau. Microb Ecol 86:2756–2769. https://doi.org/10.1007/s00248-023-02280-0

Rep M, van der Does HC, Meijer M, et al (2004) A small, cysteine-rich protein secreted by Fusarium oxysporum during colonization of xylem vessels is required for I-3-mediated resistance in tomato. Mol Microbiol 53:1373–1383. https://doi.org/10.1111/j.1365-2958.2004.04177.x

Trivedi P, Leach JE, Tringe SG, et al (2020) Plant–microbiome interactions: from community assembly to plant health. Nat Rev Microbiol 18:607–621. https://doi.org/10.1038/s41579-020-0412-1

Weller DM, Raaijmakers JM, Gardener BBM, Thomashow LS (2002) Microbial populations responsible for specific soil suppressiveness to plant pathogens. Annu Rev Phytopathol 40:309–348. https://doi.org/10.1146/annurev.phyto.40.030402.110010

Xiong W, Guo S, Jousset A, et al (2017) Bio-fertilizer application induces soil suppressiveness against Fusarium wilt disease by reshaping the soil microbiome. Soil Biology and Biochemistry 114:238–247. https://doi.org/10.1016/j.soilbio.2017.07.016

Yao B, Mou X, Li Y, et al (2025) Distinct Assembly Patterns of Soil Bacterial and Fungal Communities along Altitudinal Gradients in the Loess Plateau's Highest Mountain. Microb Ecol 88:29. https://doi.org/10.1007/s00248-025-02528-x

Zhang N, Lv F, Qiu F, et al (2023) Pathogenic fungi neutralize plant-derived ROS via Srpk1 deacetylation. EMBO J 42:e112634. https://doi.org/10.15252/embj.2022112634

Zhu J, Niu W, Zhang Z, et al (2022) Distinct roles for soil bacterial and fungal communities associated with the availability of carbon and phosphorus under aerated drip irrigation. Agricultural Water Management 274:107925. https://doi.org/10.1016/j.agwat.2022.107925

Supplementary Files

This is a list of supplementary files associated with this preprint. Click to download.

- TableS1.doc
- TableS2.doc